Cucurbitacin E inhibits the Yes-associated protein signaling pathway and suppresses brain metastasis of human non-small cell lung cancer in a murine model

PING-CHIH HSU[1-3], BO TIAN[1,4], YI-LIN YANG[1], YU-CHENG WANG[1], SHU LIU[1], ANATOLY URISMAN[5], CHENG-TA YANG[2,3], ZHIDONG XU[1], DAVID M. JABLONS[1] and LIANG YOU[1]

[1]Department of Surgery, Helen Diller Family Comprehensive Cancer Center, University of California, San Francisco, San Francisco, CA 94115, USA; [2]Department of Thoracic Medicine, Chang Gung Memorial Hospital Linkou Branch, Taoyuan 33305; [3]School of Medicine, Chang Gung University, Taoyuan 33302, Taiwan, R.O.C.; [4]Department of Thoracic Surgery, Sichuan Cancer Hospital and Institute, Sichuan Cancer Center, School of Medicine, University of Electronic Science and Technology of China, Chengdu, Sichuan 610041, P.R. China; [5]Department of Pathology, University of California, San Francisco, San Francisco, CA 94115, USA

Abstract. Human non-small cell lung cancer (NSCLC) is associated with an extremely poor prognosis especially for the 40% of patients who develop brain metastasis, and few treatment strategies exist. Cucurbitacin E (CuE), an oxygenated tetracyclic triterpenoid isolated from plants particularly of the family Cucurbitaceae, has shown anti-tumorigenic properties in several types of cancer, yet the mechanism remains unclear. Yes-associated protein (YAP), a main mediator of the Hippo signaling pathway, promotes tumorigenesis, drug resistance and metastasis in human NSCLC. The present study was designed to ascertain whether CuE inhibits YAP and its downstream gene expression in the human NSCLC cell lines H2030-BrM3 (K-ras^{G12C} mutation) and PC9-BrM3 (EGFR$^{\Delta exon19}$ mutation), which have high potential for brain metastasis. The efficacy of CuE in suppressing brain metastasis of H2030-BrM3 cells in a murine model was also investigated. It was found that after CuE treatment in H2030-BrM3 and PC9-BrM3 cells, YAP protein expression was decreased, and YAP signaling GTIIC reporter activity and expression of the downstream genes CTGF and CYR61 were significantly (P<0.01) decreased. CuE treatment also reduced the migration and invasion abilities of the H2030-BrM3 and PC9-BrM3 cells. Finally, our *in vivo* study showed that CuE treatment (0.2 mg/kg) suppressed H2030-BrM3 cell brain metastasis and that mice treated with CuE survived longer than the control mice treated with 10% DMSO (P=0.02). The present study is the first to demonstrate that CuE treatment inhibits YAP and the signaling downstream gene expression in human NSCLC *in vitro*, and suppresses brain metastasis of NSCLC in a murine model. More studies to verify the promising efficacy of CuE in inhibiting brain metastasis of NSCLC and various other cancers may be warranted.

Introduction

Brain metastasis affects approximately 40% of patients with non-small cell lung cancer (NSCLC) (1,2). The prognosis for these patients is extremely poor; median survival is less than three months without treatment (3,4). Treatment options for those patients whose tumors lack targetable mutations remain quite limited. For example, erlotinib, an epidermal growth factor receptor (EGFR)-tyrosine kinase inhibitor (TKI), is an effective target therapy for brain metastatic lung adenocarcinoma harboring EGFR exon 19 deletion or exon 21 L858R mutations (5-8). Anaplastic lymphoma kinase (ALK) inhibitors including ceritinib and alectinib have better response rates than conventional chemotherapy for brain metastatic NSCLC patients with ALK-rearrangement mutation (9,10). Although the K-ras mutation is common in NSCLC patients (15-30%), there is still no approved target therapy drug for K-ras mutant metastatic NSCLC (11,12). There is therefore an important need to develop novel drugs for the treatment of brain metastatic NSCLC patients without targetable driven mutations.

Cucurbitacin E (CuE, a-elaterin) (Fig. 1A) is a tetracyclic triterpene and a biochemical natural compound from the family of cucurbitacins. CuE can be isolated from natural plants such as those of the family Cucurbitaceae (gourd,

Correspondence to: Dr Liang You, Department of Surgery, Helen Diller Family Comprehensive Cancer Center, University of California, San Francisco, 2340 Sutter Street, N-221, San Francisco, CA 94115, USA
E-mail: liang.you@ucsf.edu

Abbreviations: CuE, cucurbitacin E; NSCLC, non-small cell lung cancer; YAP, Yes-associated protein; CHX, cycloheximide

cucumber, pumpkins) (13). Previous studies have shown that CuE inhibits the proliferation, invasion and migration abilities of various types of cancers, including lung, colorectal and breast, yet the mechanism by which it performs these functions and the signaling pathway remain unclear (13-19).

Yes-associated protein (YAP) is a key mediator protein in the Hippo (also known as the Salvador-Warts-Hippo) signaling pathway, and is reportedly an important oncogenic protein in various types of cancer (20,21). Recently, YAP was found to promote tumorigenesis, invasion, drug resistance, brain metastasis and immune evasion in human NSCLC (22-28). Thus, YAP has been suggested as a therapeutic target for metastatic NSCLC. However, to date, no molecular inhibitor targeting YAP has been developed for the treatment of NSCLC. Therefore, identification of a natural biochemical compound that can inhibit the YAP signaling pathway is an alternative strategy.

In the present study, we sought to determine whether CuE inhibits YAP expression in the NSCLC cell lines H2030-BrM3 (K-ras^{G12C} mutation) and PC9-BrM3 (EGFR$^{\Delta exon19}$ mutation), which have high potential for brain metastasis. We also investigated the efficacy of CuE in suppressing human NSCLC brain metastasis in a murine model.

Materials and methods

Cell culture. Human metastatic NSCLC cell lines H2030-BrM3 (K-ras^{G12C} mutation) (P9) and PC9-BrM3 (EGFR$^{\Delta exon19}$ mutation) (P40) were gifts from Professor Joan Massagué (Metastasis Research Center, Memorial Sloan Kettering Cancer Center, New York, NY, USA). The H2030-BrM3 and PC9-BrM3 cell lines are *in vivo* selection of metastatic derivatives from NCI-H2030 (K-ras^{G12C} mutation) and PC9 cell lines (EGFR$^{\Delta exon19}$ mutation). The two cell lines were derived and authenticated by left ventricle inoculation as previously described (29,30). Cells were maintained in RPMI-1640 medium supplemented with 10% heat-inactivated fetal bovine serum (FBS) and streptomycin (100 mg/ml) (UCSF Cell Culture Facility, San Francisco, CA, USA), and cultured at 37°C in a humid incubator with 5% CO_2.

Animal studies. All animal studies strictly followed UCSF institutional guidelines (Institutional Animal Care and Use Committee approval no. AN103205-03). Twenty athymic nude (CrTac:NCr-Foxn1^{nu}) female mice, 6-8 weeks of age (body weight at ~20 g) were purchased from Taconic Farms, Inc. (Hudson, NY, USA) and maintained in ventilated cages (with reach food and water) at a constant temperature (20-22°C) and a 12 h light dark cycle in UCSF's Laboratory Animal Resource Center (LARC) facility. The murine experiments were initiated when mice were older than 10 weeks. A metastatic murine model was created by injecting 500,000 H2030-BrM3 cells suspended in 100 μl of PBS into the left ventricle via a percutaneous approach as previously described (29,30). To test whether cucurbitacin E (CuE) (Sigma Aldrich; Merck KGaA) could control NSCLC cell line H2030-BrM3 metastasis in our murine model, mice were divided into two groups of n=10 each. The control group was administered an intraperitoneal (i.p.) injection of 10% dimethyl sulfoxide (DMSO), and the treatment group was administered an i.p. injection of 0.2 mg/kg of CuE. Both treatments began on the day following

cell injection and were administered every other day. The mice were euthanized when they showed symptoms of paralysis, appeared extremely sick or a tumor size exceeding 2 cm^3, according to the guidelines established by the UCSF LARC and tumor tissues were collected. Survival was assessed from the day of cell injection to the day mice were euthanized.

To monitor the condition of brain metastasis in the mice, bioluminescent imaging (Caliper Life Sciences, Waltham, MA, USA) was used. For this, mice were injected with D-luciferin potassium salt (SYD Labs, Inc., Natick, MA, USA) at a dose of 150 mg/kg i.p., anesthetized by inhalant isoflurane 1-5% in oxygen, and then placed into the Xenogen IVIS® spectrum imaging system (PerkinElmer, Boston, MA, USA) at 10 min after D-luciferin potassium salt injection. Images were recorded with an exposure time of 1 min.

Cell viability assay. H2030-BrM3 and PC9-BrM3 cells were cultured in a 96-well plate and treated with different doses of CuE (Sigma Aldrich; Merck KGaA) (0, 0.01, 0.03, 0.1, 0.3, 1, 3, 10, 30 and 100 μM). After 72 h of incubation, the cells were lysed and CellTiter-Glo Luminescent Cell Viability Assay reagent (Promega) was added to generate luminescent signaling. Luminescent signaling was detected by using the GloMax-96 Microplate Luminometer (Promega, Madison, WI, USA). GraphPad Prism 5.0 software (GraphPad Software, Inc., La Jolla, CA, USA) was used to analyze proportional cell viability and calculate dose-response curves and the half maximal inhibitory concentration (IC$_{50}$) value.

Luciferase gene transfection. The pGreenFire1-CMV Virus (pTRH1 CMV dscGFP T2A Fluc) positive control was purchased from System Bioscience LLC (Palo Alto, CA, USA). Virus particles were mixed with transfection reagents and medium according to the manufacturer's protocol, and added to the H2030-BrM3 cells cultured in 12-well plates. Fluorescence microscopy was used to determine the efficacy of transfection at 48 h after transfection.

Western blot analysis. The samples were run on 4-20% gradient SDS-polyacrylamide gels (Bio-Rad Laboratories, Inc., Hercules, CA, USA) and then were transferred to Immobilon-P nitrocellulose membranes (Millipore, Bellerica, MA, USA). The membranes were probed with the following primary antibodies: Rabbit anti-YAP (Cell Signaling, cat. no. 4912; dilution 1:1,000), anti-ERK1/2 (Cell Signaling, cat. no. 4912; dilution 1:1,000) and mouse anti-GAPDH (Sigma-Aldrich; Merck KGaA; cat. no. 100242-MM05; dilution 1:10,000) at 4°C overnight after blocking with 5% non-fat milk. The membranes were then incubated with species-specific conjugated secondary antibodies (GE Dharmacon) (cat. no. NA934, anti-rabbit for YAP; cat. no. NA931, anti-mouse for GAPDH) at room temperature for 1 h. Finally, an ECL blotting analysis system (Amersham Pharmacia Biotech, Piscataway, NJ, USA) was used to detect protein expression.

Protein degradation assay. H2030-BrM3 and PC9-BrM3 cells were placed in 6-well plates, and treated with either 0.1 μM CuE or DMSO (control). After 24 h of treatment, the cells were treated with 100 μg/ml cycloheximide (CHX) (Sigma-Aldrich; Merck KGaA), an inhibitor of protein synthesis. Cells were

harvested at the time points of 0, 1 and 2 h after CHX treatment. Total proteins were extracted and YAP expression was analyzed by western blot analysis.

Luciferase reporter assay. The cell lines H2030-BrM3 and PC9-BrM3 were placed in 24-well plates and transfected with 8xGTIIC-luciferase plasmid (Addgene, Cambridge, MA, USA) and *Renilla* luciferase pRL-TK plasmid (Promega, Madison, WI, USA) by using transfection reagent Lipofectamine 2000 (Invitrogen; Thermo Fisher Scientific, Inc.). At 24 h after transfection, the cells were treated with CuE. After a 24 h treatment, the cells were lysed and luciferase activity was assayed by using Dual-Luciferase Reporter Assay system (Promega). Luminescent signaling was detected by using GloMax-96 Microplate Luminometer. All luciferase activities were normalized to *Renilla* activity. All experiments of luciferase reporter assay were triplicated to achieve statistical significance [DMSO (n=3), CuE 0.05 μM (n=3), CuE 0.1 μM (n=3)].

RNA isolation, cDNA synthesis, and quantitative real-time RT-PCR. Total RNA was extracted from cells by using the High Pure RNA Isolation Kit (Roche, Indianapolis, IN, USA). The iScript cDNA Synthesis Kit (Bio-Rad Laboratories, Inc.) was used to transcribe RNA to cDNA, and the cDNA was used as the template for real-time PCR. Commercially available primers and probe sequences (Applied Biosystems; Thermo Fisher Scientific, Inc.) were used to detect YAP, CYR61, CTGF, EREG and endogenous control gene β-glucuronidase (GUSB) gene expression. Applied Biosystems Relative Quantification software (Version C; Thermo Fisher Scientific, Inc.) was used for mRNA expression analysis. Real-time PCR detection was conducted using TaqMan Technology on an Applied Biosystems 7000 sequence detection system (Thermo Fisher Scientific, Inc.). All experiments of real-time RT-PCR were triplicated to achieve statistical significance [DMSO (n=3), CuE 0.05 μM (n=3), CuE 0.1 μM (n=3)].

Wound-healing and Transwell invasion assay. For the wound-healing migration assay, H2030-BrM3 and PC9-BrM3 cells were subcultured in 6-well plates until the condition of confluence was reached. The plates were scratched using a 200 μl pipette tip, and the cells were grown continuously. In a test of CuE treatment, 0.05 μM was added after the scratch. Phase contrast images were captured at the time of the scratch (0 h) and 18 h later with a Primo Vert microscope (magnification x100, x200 and x400, respectively; Carl Zeiss, Gottingen, Germany), and the distance of cell movement was measured by ImageJ software (National Institutes of Health, Bethesda, MD, USA).

The 6-well plate Transwell system used for the Transwell invasion assay was purchased from Corning Inc. (Corning, NY, USA). The upper chamber of the Transwell plate was coated with 300 μl mMatrigel. Next, H2030-BrM3 and PC9-BrM3 cells were trypsinized and re-suspended in serum-free medium and the cells were seeded on the upper chamber of the Transwell plate. CuE (0.05 μM) was added with serum-free medium to the upper chamber. The lower chamber was infused with 2 ml complete growth medium (10% FBS). The gel in the upper chamber of the Transwell plate was wiped after incubation

at 37˚C for 48 h. The membrane of the upper chamber was stained by crystal violet for 10 min after methanol fixation. The Primo Vert microscope was again used to observe the cells on the lower side of the membrane, and phase contrast images were captured at x100, x200 and x400 magnification.

Wound-healing and Tanswell invasion assays were triplicated to achieve statistical significance [DMSO (n=3, CuE 0.05 μM (n=3)].

Histologic analysis and immunohistochemistry. After mice were euthanized, the tumor tissues from brain metastases were harvested, immediately fixed in 10% paraformaldehyde for 24 h and then embedded in paraffin. Histological sections of the tissues were stained with hematoxylin and eosin (H&E) stain for general morphological analysis. The morphological analysis to verify brain metastasis in the stained tissues was performed by an experienced pathologist. The YAP immunohistochemistry (IHC) staining was conducted as previously described (27). All images were obtained using a Zeiss Axioscop 2 microscope at x100, x200 and x400 magnification (Carl Zeiss Inc.).

Statistical analysis. All statistical analyses were conducted using GraphPad Prism (version 5.0; GraphPad Software, San Diego, CA, USA). Data are expressed as mean ± standard deviation (SD) from three independent experiments. t-tests were used to compare the differences between two groups, and one-way ANOVA followed by Turkey multiple comparisons was used to compare differences among >2 groups. A Kaplan-Meier survival curve was calculated to determine survival in the animal experiments. The experiments of reporter assay, real-time RT-PCR, wound-healing and Transwell invasion assays were triplicated to achieve statistical significance. All P-values were 2-sided and considered to be statistically significant at P<0.05 (*P<0.05, **P<0.01, ***P<0.001 as indicated in the figures and legends).

Results

CuE decreases YAP protein expression in H2030-BrM3 and PC9-BrM3 cells. The cell viability assay of H2030-BrM3 and PC9-BrM3 cells treated with CuE yielded IC_{50} values of 0.146 and 0.187 μM, respectively (Fig. 1B and C). Western blotting showed that the level of YAP protein was decreased after treatment with 0.05 and 0.1 μM CuE in the H2030-BrM3 and PC9-BrM3 cells when compared to the DMSO control (Fig. 1D). The YAP protein degradation assay showed that in H2030-BrM3 and PC9-BrM3 cells treated with 0.1 μM CuE, YAP protein expression reached low levels at 2 h when compared to the DMSO-treated controls (Fig. 1E). Real-time PCR showed that YAP mRNA expression was significantly decreased in the H2030-BrM3 and PC9-BrM3 cell lines after treatment with 0.05 (P<0.001 and P<0.01) and 0.1 μM CuE (both P<0.001) when compared with the DMSO control (Fig. S1A and B). Western blot analysis showed that ERK1/2 protein was significantly decreased after treatment with 0.05 and 0.1 μM CuE in the H2030-BrM3 and PC9-BrM3 cell lines (Fig. S1C and D).

CuE decreases GTIIC reporter activity and YAP downstream gene mRNA expression. After verifying that CuE decreases
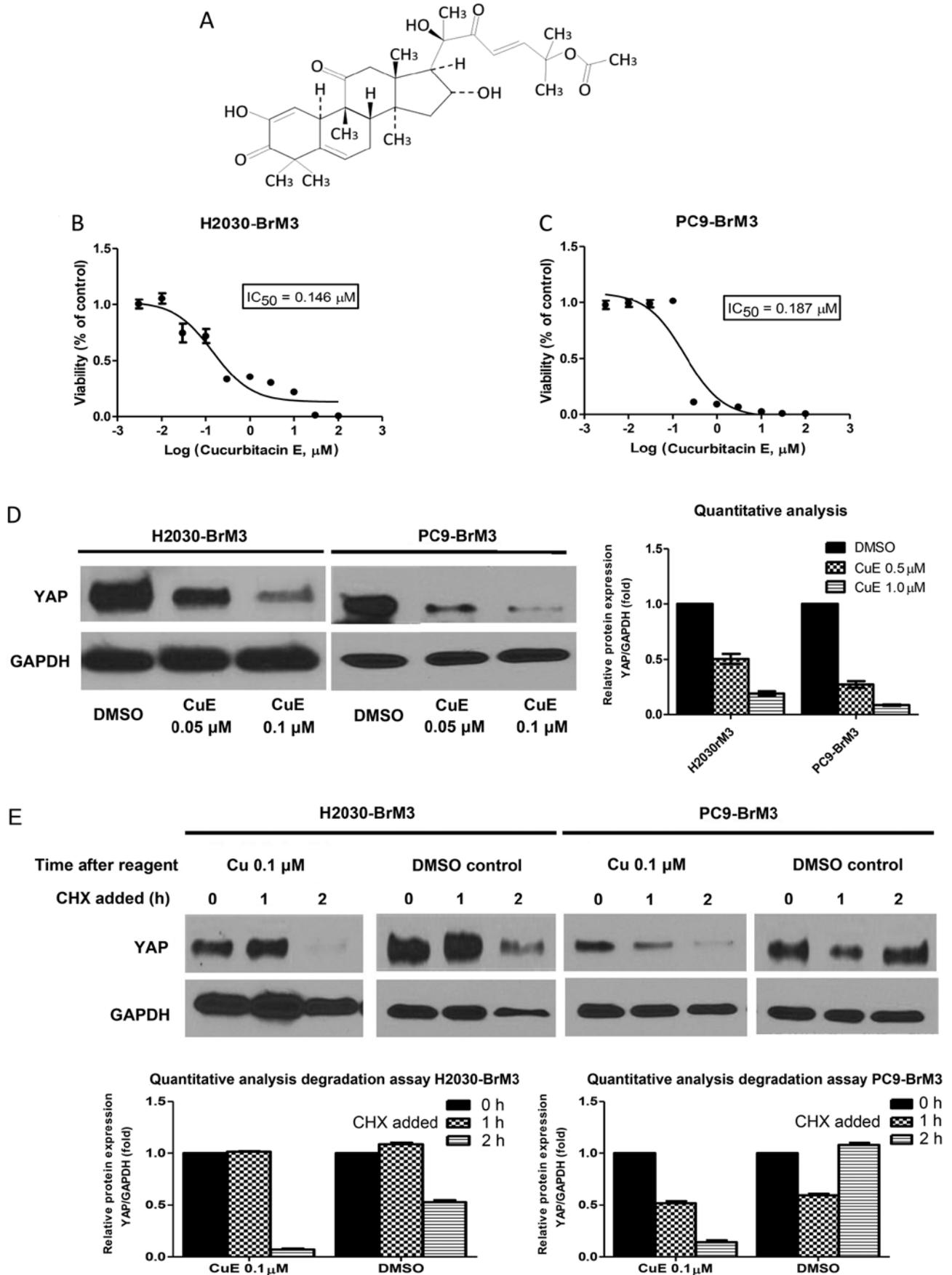
Figure 1. CuE decreases YAP protein in H2030-BrM3 and PC9-BrM3 cell lines. (A) Chemical structure of CuE. Cell viability analysis in (B) H2030-BrM3 and (C) PC9-BrM3 cells after CuE treatment. (D) YAP protein level was decreased in H2030-BrM3 and PC9-BrM3 cell lines after 0.05 and 0.1 μM CuE treatment when compared to the DMSO control. (E) YAP protein degradation assay showed that YAP protein was degraded more rapidly after 0.1 μM CuE treatment when compared with the DMSO control. CuE, cucurbitacin E; IC_{50}, half maximal inhibitory concentration; CHX, cycloheximide; DMSO, dimethyl sulfoxide; YAP, Yes-associated protein.
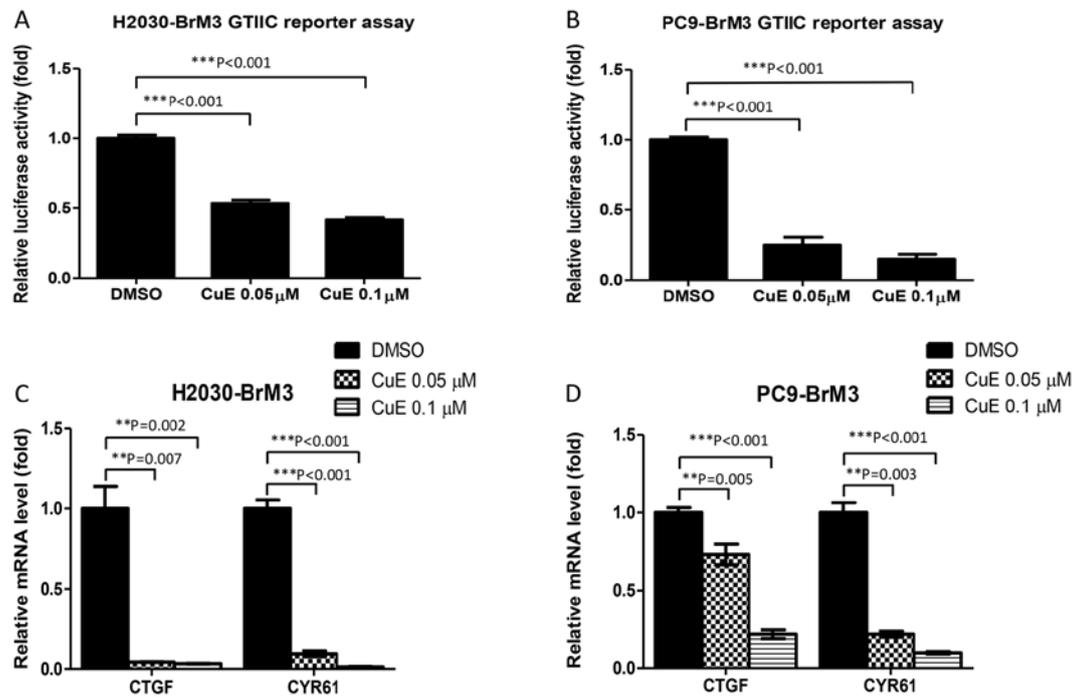
Figure 2. Hippo reporter activity and downstream gene expression are decreased after 0.05 and 0.1 μM CuE treatment in H2030-BrM3 and PC9-BrM3 cells. GTIIC reporter activity was significantly decreased after 0.05 and 0.1 μM CuE treatment in (A) H2030-BrM3 and (B) PC9-BrM3 cell lines. *CTGF* and *CYR61* mRNA expression was significantly decreased after either dose of CuE in the (C) H2030-BrM3 and (D) PC9-BrM3 cell lines. Error bars indicate standard deviations; **P<0.01, ***P<0.001 when compared to the DMSO control. CuE, cucurbitacin E; DMSO, dimethyl sulfoxide.

YAP protein expression in H2030-BrM3 and PC9-BrM3 cells, we ascertained whether it could also decrease GTIIC reporter activity and YAP downstream gene mRNA expression. We demonstrated that GTIIC reporter activity in the H2030-BrM3 and PC9-BrM3 cell lines was significantly decreased after 0.05 and 0.1 μM CuE treatment compared to the DMSO control (all P<0.001) (Fig. 2A and B). In both cell lines, mRNA expression of the YAP downstream genes CTGF and CYR61 was significantly decreased after 0.05 and 0.1 μM CuE treatment (P<0.01) (Fig. 2C and D), as was mRNA expression of epidermal growth factor (EGF), epiregulin (EREG) (P<0.05) (Fig. S1E and F).

CuE reduces migration and invasion abilities of H2030-BrM3 and PC9-BrM3 cells. To investigate whether CuE could reduce the migration and invasion abilities of H2030-BrM3 and PC9-BrM3 cells, we used wound closure and Transwell invasion assays. The migration assay showed that the wound closure rate was significantly decreased in the H2030-BrM3 and PC9-BrM3 cells after 0.05 μM CuE treatment (P<0.01 and P<0.001) when compared with the DMSO control (Fig. 3A-D). The Transwell invasion assay showed that the number of cells that invaded the lower side of the membrane was significantly decreased in both cell lines after 0.05 μM CuE treatment (P<0.01) when compared to the DMSO control (Fig. 3E-H) (Fig. S2).

CuE decreases the burden of brain metastasis in an in vivo H2030-BrM3 cell murine model of brain metastasis. To test the efficacy of CuE in suppressing brain metastasis of H2030-BrM3 cells *in vivo*, mice were inoculated with H2030-BrM3 cells through percutaneous left ventricle injection and then treated with CuE at a dose of 0.2 mg/kg. Control mice were treated with 10% DMSO. Bioluminescent imaging showed that mice treated with CuE had significantly decreased brain metastatic burden compared to the control group at day 35 (week 7) (P=0.034 (Fig. 4A and B). Mice treated with CuE survived significantly longer than those treated with 10% DMSO (P=0.0212) (Fig. 4C).

CuE decreases nuclear YAP immunohistochemical (IHC) staining of mouse brain tumor tissue. After mice were euthanized, brain tissues were collected from the DMSO control and CuE-treated groups for histological analysis. H&E staining was assayed to verify that H2030-BrM3 tumor cell metastasis appeared in the mouse model. Metastasis of H2030-BrM3 tumor cells within brain tissues could be observed by H&E staining (Fig. 5A). To observe the late effect of CuE treatment on YAP in regards to brain metastasis, nuclear YAP IHC staining was performed. The results showed that nuclear YAP IHC staining was decreased in the brain tissue of the CuE-treated group when compared to that observed in the brain tissue of the control DMSO group (Fig. 5B).

Discussion

Although the natural biochemical compound CuE has been shown to inhibit the proliferation, invasion and migration abilities of various types of cancer, the mechanism and the signaling pathway remain unclear, until now. Our study revealed that CuE inhibited YAP protein expression in the NSCLC cell lines H2030-BrM3 and PC9-BrM3, which were derived from NSCLC cell lines NCI-H2030 (K-ras^{G12C} mutation) and
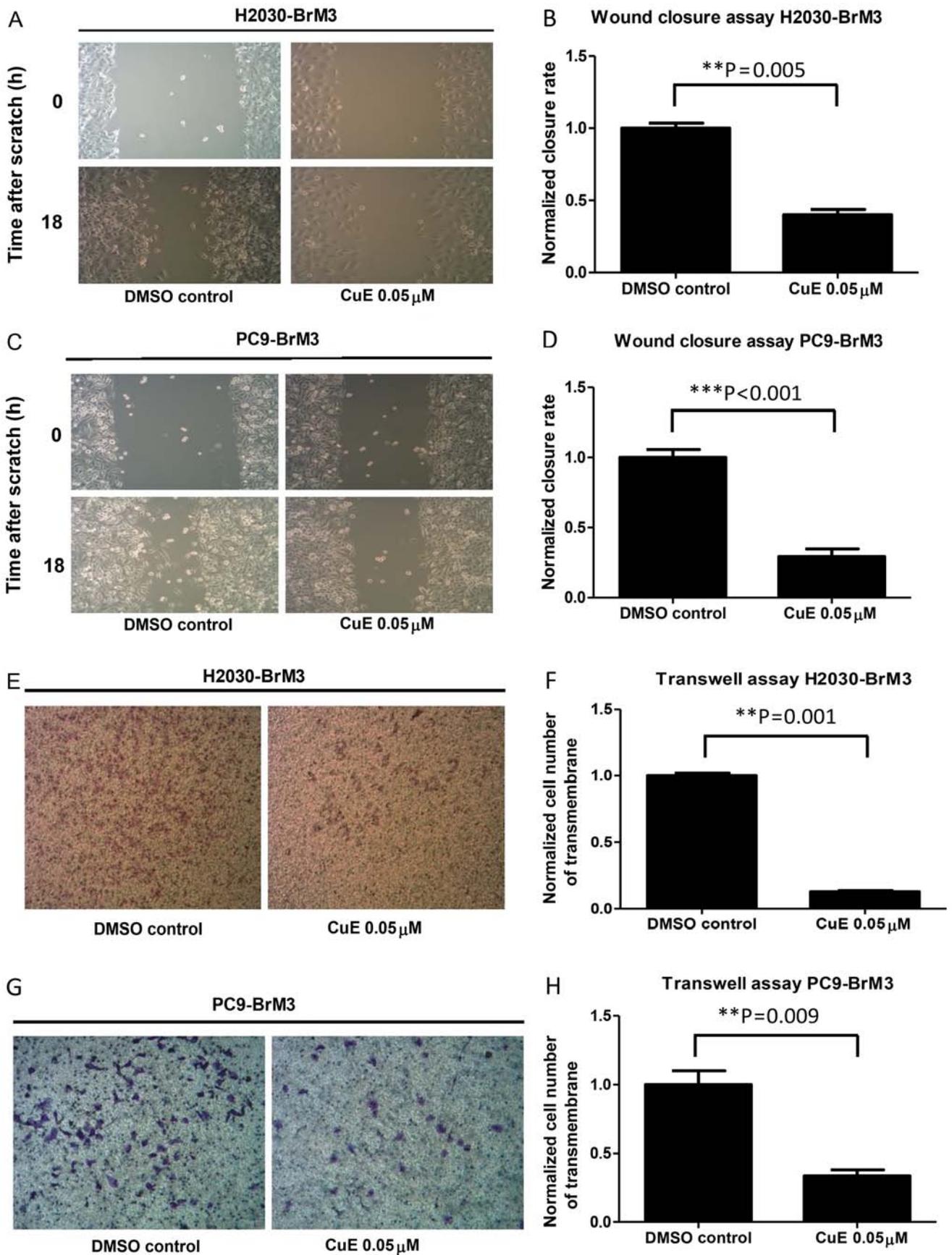
Figure 3. Analysis of cell migration and invasion abilities of H2030-BrM3 and PC9-BrM3 cells after CuE treatment. Decrease in cell migration ability in the (A) H2030-BrM3 and (C) PC9-BrM3 cells after 0.05 μM CuE treatment. (B and D) Quantitative analysis of migration assay result, indicating CuE treatment significantly decreased cell migration ability. Decrease in cell invasion ability in the (E) H2030-BrM3 and (G) PC9-BrM3 cells after 0.05 μM CuE treatment. (F and H) Quantitative analysis of the Transwell invasion assay result, indicating that 0.05 μM CuE treatment decreased cell invasion ability in the H2030-BrM3 and PC9-BrM3 cells. Error bars indicate standard deviations; $^{**}P<0.01$, $^{***}P<0.001$, when compared to the DMSO control. CuE, cucurbitacin E; DMSO, dimethyl sulfoxide.
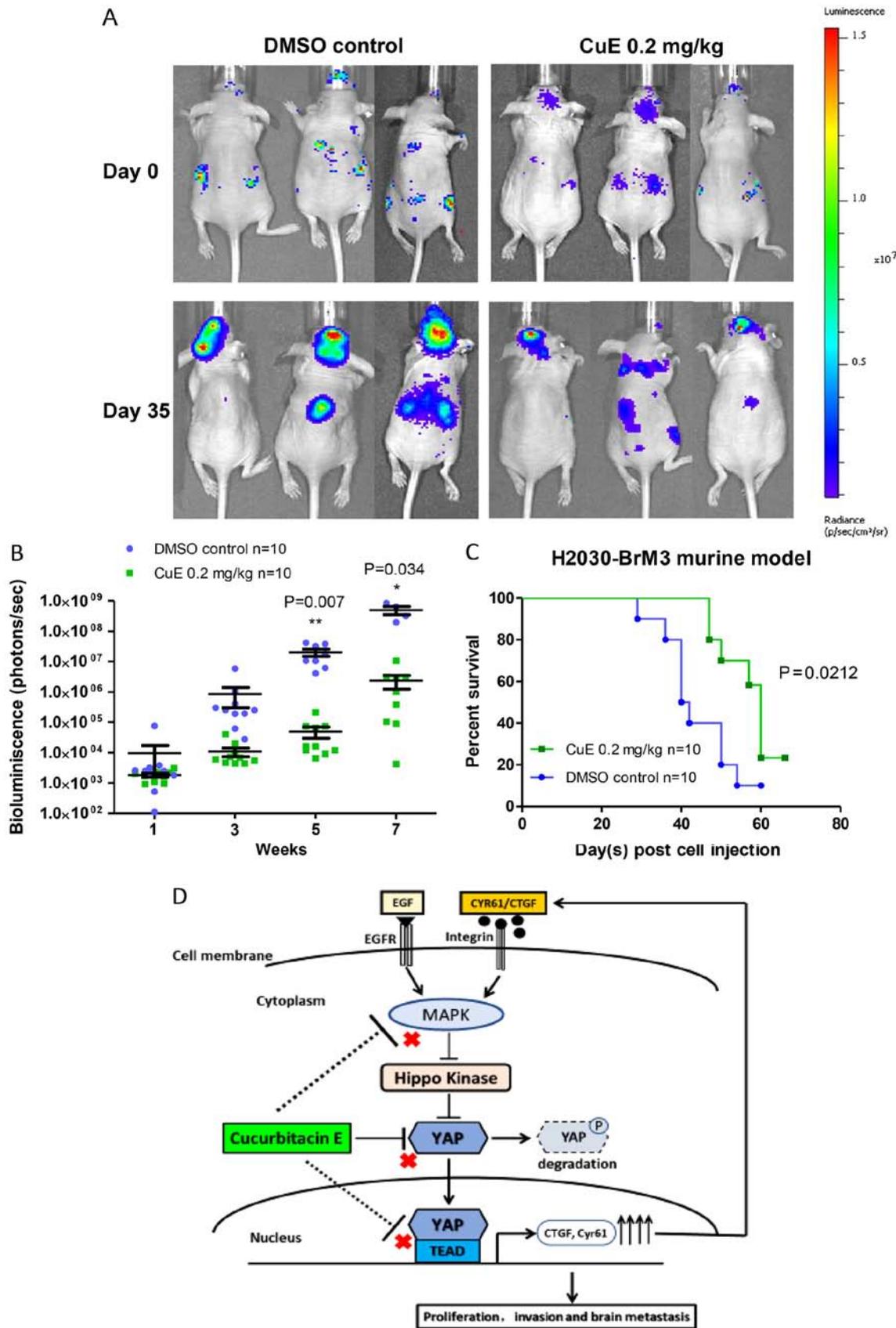
Figure 4. CuE treatment suppresses brain metastasis of H2030-BrM3 cells in a murine model (control 10% DMSO n=10, CuE treatment 0.2 mg/kg n=10). (A) Bioluminescence images of mice treated with CuE and DMSO. (B) Tumor metastasis burden in control mice and mice treated with CuE based on photon flux (photons per second) (P=0.007 at 5 weeks and P=0.034 at 7 weeks). (C) Kaplan-Meier survival curves for control and CuE-treated mice (P=0.0212). (D) Hypothetical model of our study. In H2030-BrM3 cells, activation of YAP increased the mRNA expression of downstream genes *CTGF* and *CYR61*, which form an autocrine loop to enhance the MAPK signaling pathway. This enhancement increased the invasion and migration abilities and the metastatic potential of H2030-BrM3 cells. CuE treatment inhibited YAP protein expression, and possibly also inhibited YAP at the transcriptional level. Therefore, CuE inhibited the brain metastasis of H2030-BrM3 cells by inhibiting the YAP signaling pathway. CuE, cucurbitacin E; DMSO, dimethyl sulfoxide; YAP, Yes-associated protein.
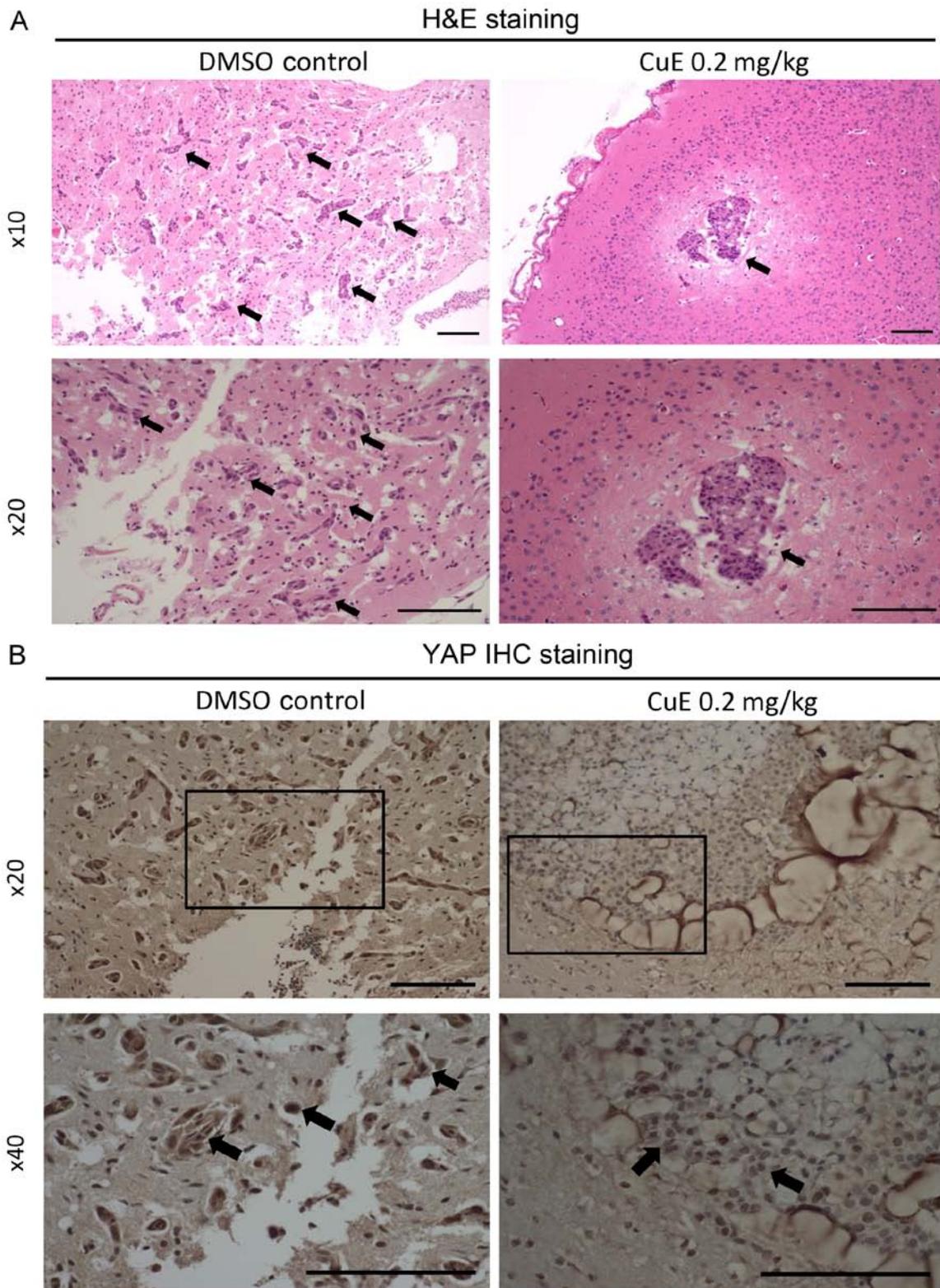
Figure 5. Histological analysis of the mouse brain tissue (control 10% DMSO n=3, CuE treatment 0.2 mg/kg n=3). (A) H&E staining was performed to verify that brain metastasis of H2030-BrM3 cells appeared in the mouse model. Arrows point to the metastatic tumors in brain tissues from control mice and mice treated with CuE. (B) Nuclear YAP immunohistochemical (IHC) staining was conducted to observe the late effect of CuE treatment. The results showed that nuclear YAP IHC staining was decreased in the brain tissues of the CuE-treated group when compared to the tissues in the DMSO control group (arrows point to the nuclear YAP IHC staining). Scale bar, 100 μm. H&E, hematoxylin and eosin; CuE, cucurbitacin E; DMSO, dimethyl sulfoxide; YAP, Yes-associated protein.

PC9 (EGFR$^{\Delta exon19}$ mutation), which show very strong brain metastatic potential in murine experiments (27,29). We verified that CuE decreases YAP GTIIC Hippo reporter activity, and expression of the downstream genes connective tissue growth factor (CTGF) and cysteine-rich angiogenic inducer 61 (CYR61). Collectively, these results suggest that CuE inhibits tumorigenesis, invasion and migration thorough inhibition of the YAP signaling pathway.

PC9-BrM3 cells contain an EGFR$^{\Delta exon19}$ mutation and depend on the EGFR/mitogen-activated protein kinase (MAPK)/extracellular signal-regulated kinase (ERK) signaling pathway to maintain tumor survival. PC9-BrM3 cells are sensitive to EGFR-tyrosine kinase inhibitor treatment (27,29,30). Although H2030-BrM3 cells have a K-ras^{G12C} mutation, previous studies suggest that these cells do not fully depend on the EGFR/RAS/MAPK/ERK signaling pathway to maintain tumor survival (27,31). In addition, YAP has been suggested to be an oncogenic protein that partly takes over the K-ras mutation in H2030-BrM3 cells (27,31). These findings may explain why YAP protein expression did not decrease equally after CuE treatment in the two cell lines.

Our experimental data showed that CuE treatment decreased YAP mRNA expression, ERK1/2 protein expression, and epidermal growth factor (EGF) EREG mRNA expression in H2030-BrM3 and PC9-BM3 cells. These results suggest that CuE inhibits YAP, at least in part, indirectly through the EGFR/MAPK/ERK signaling pathway. Previous studies have reported crosstalk between the Hippo/YAP and EGFR/MAPK/ERK signaling pathways in human NSCLC cells (22,24,32). Increased cytoplasmic YAP protein translocates into the nucleus to form complexes with transcriptional enhancer factors (TEF; also known as TEAD) leading to activate transcription of downstream genes including CTGF, CYR61 and EGF such as EREG (22,24,27,32). Therefore, YAP regulates these downstream genes, including CTGF, CYR61 and EREG, at the transcriptional mRNA level, not at the protein level. The increased expression of CTGF, CYR61 and EREG may form an autocrine loop with the EGFR/MAPK/ERK signaling pathway to re-enforce YAP protein expression. Two studies demonstrated that CuE inhibits the EGFR/MAPK/ERK signaling pathway in cancer cells (33,34). Recently, CuB was shown to inhibit the Hippo/YAP pathway in human colorectal cancer cell lines (35). These findings lead us to believe that CuE inhibits YAP indirectly through the EGFR/MAPK/ERK and Hippo/YAP signaling pathways in human NSCLC. Further studies in the future to investigate the effects of CuE on ErbB family receptors (EGFR, HER2, ErbB3 and HER4)/MAPK/ERK signaling pathway and Hippo kinase including neurofibromatosis 2 (NF2), large tumor suppressor homolog 1 (LATS1), LATS2, and mammalian sterile-20 like kinase 1 (MST1) in various cancers are suggested according to our findings. The dependence on the EGFR/MAPK/ERK signaling pathway of PC9-BrM3 cells may explain why more YAP protein was decreased and degraded after CuE treatment in that cell line when compared with that observed in the H2030-BrM3 cells.

Several studies have shown that CuE has anticancer activity to NSCLC by inhibiting oncogenic signaling pathways, including the Wnt signaling pathway and the Janus kinase (JAK)/signal transducer and activator of transcription 3 (STAT3) signaling pathway (15,36,37). Wnt and STAT3 signaling pathways were reportedly involved in regulating the expression of Hippo downstream genes CTGF and CYR61 (38-41). Collectively, these findings may explain why the decrease of 50-80% in YAP protein by CuE treatment resulted in more than 90% of CTGF and CYR61 mRNA expression in H2030-BrM3 cells in our study.

According to several reports, YAP takes over KRAS as a cancer driver in KRAS-mutant NSCLC, and promotes cancer metastasis in NSCLC (41-45). A recent study found that K-ras mutant H2030-BrM3 cells have increased YAP protein and YAP downstream genes CTGF and CYR61 mRNA expressions compared with parental H2030 cells (27). In that study, direct inhibition of YAP by short hairpin RNA suppressed brain metastasis of H2030-BrM3 cells in a mouse model. After verifying that CuE inhibits YAP signaling *in vitro*, we explored the efficacy of CuE in suppressing brain metastasis of H2030-BrM3 cells in a mouse model (Fig. 4D).

Our study is the first to show that CuE suppresses brain metastasis of human NSCLC in a murine model. A recent study showed that cucurbitacin B (another tetracyclic cucurbitane) inhibits the Hippo-YAP signaling pathway in colorectal cancer cells, but included no *in vivo* data (35). Another study demonstrated that CuE inhibited breast cancer in a mouse model of metastasis by suppressing cell migration and invasion, but the anti-cancer mechanism of CuE was not investigated (18).

In conclusion, our study revealed that the anti-tumorigenic effects of CuE occur through inhibition of the YAP signaling pathway, and that CuE treatment suppressed brain metastasis of human NSCLC cells in a murine model. More studies to verify the promising efficacy of CuE in inhibiting brain metastasis of NSCLC and various other cancers may be warranted.

Availability of data and materials

The datasets used during the present study are available from the corresponding author upon reasonable request.

Authors' contributions

Conception and design was accomplished by PCH and LY. Development of the research methodology was carried out by PCH, ZX and YLY. Acquisition of data (as well as provision of research animals and facilities) was accomplished by PCH, BT, SL and DMJ. Analysis and interpretation of data (pathologic analysis) was carried out by PCH, BT, ZX and AU.

Writing, review and/or revision of the manuscript was carried out by PCH, BT, YLY, CTY and LY. Administrative, technical, or material support (organizing data) was achieved by PCH, BT, YLY, YCW, ZX and LY. Study supervision was carried out by LY. All authors read and approved the manuscript and agree to be accountable for all aspects of the research in ensuring that the accuracy or integrity of any part of the work are appropriately investigated and resolved.

Ethics approval and consent to participate

All animal studies strictly followed UCSF institutional guidelines (Institutional Animal Care and Use Committee approval no. AN103205-03).

Patient consent for publication

Not applicable.

Competing interests

All authors have no competing interest.

References

1. Duell T, Kappler S, Knöferl B, Schuster T, Hochhaus J, Morresi-Hauf A, Huber RM, Tufman A and Zietemann V: Prevalence and risk factors of brain metastases in patients with newly diagnosed advanced non-small-cell lung cancer. Cancer Treat Commun 4: 106-112, 2015.
2. Ma X, Zhu H, Guo H, Han A, Wang H, Jing W, Zhang Y, Kong L and Yu J: Risk factors of brain metastasis during the course of EGFR-TKIs therapy for patients with EGFR-mutated advanced lung adenocarcinoma. Oncotarget 7: 81906-81917, 2016.
3. Sørensen JB, Hansen HH, Hansen M and Dombernowsky P: Brain metastases in adenocarcinoma of the lung: Frequency, risk groups, and prognosis. J Clin Oncol 6: 1474-1480, 1988.
4. Dempke WC, Edvardsen K, Lu S, Reinmuth N, Reck M and Inoue A: Brain metastases in NSCLC-are TKIs changing the treatment strategy? Anticancer Res 35: 5797-5806, 2015.
5. Deng Y, Feng W, Wu J, Chen Z, Tang Y, Zhang H, Liang J, Xian H and Zhang S: The concentration of erlotinib in the cerebrospinal fluid of patients with brain metastasis from non-small-cell lung cancer. Mol Clin Oncol 2: 116-120, 2014.
6. Paz-Ares L, Soulières D, Moecks J, Bara I, Mok T and Klughammer B: Pooled analysis of clinical outcome for EGFR TKI-treated patients with EGFR mutation-positive NSCLC. J Cell Mol Med 18: 1519-1539, 2014.
7. Taniguchi Y, Tamiya A, Nakahama K, Naoki Y, Kanazu M, Omachi N, Okishio K, Kasai T and Atagi S: Impact of metastatic status on the prognosis of EGFR mutation-positive non-small cell lung cancer patients treated with first-generation EGFR-tyrosine kinase inhibitors. Oncol Lett 14: 7589-7596, 2017.
8. Li K, Yang M, Liang N and Li S: Determining EGFR-TKI sensitivity of G719X and other uncommon EGFR mutations in non-small cell lung cancer: Perplexity and solution (Review). Oncol Rep 37: 1347-1358, 2017.
9. Cao Z, Gao Z, Fu M, Ni N, Pei Y and Ou WB: Anaplastic lymphoma kinase fusions: Roles in cancer and therapeutic perspectives. Oncol Lett 17: 2020-2030, 2019.
10. Khan M, Lin J, Liao G, Tian Y, Liang Y, Li R, Liu M and Yuan Y: ALK inhibitors in the treatment of ALK positive NSCLC. Front Oncol 8: 557, 2019.
11. Saber A, van der Wekken A, Hiltermann TJ, Kok K, Van den Berg A and Groen H: Genomic aberrations guiding treatment of non-small cell lung cancer patients. Cancer Treat Commun 4: 23-33, 2015.
12. Tan WL, Jain A, Takano A, Newell EW, Iyer NG, Lim WT, Tan EH, Zhai W, Hillmer AM, Tam WL and Tan DSW: Novel therapeutic targets on the horizon for lung cancer. Lancet Oncol 17: e347-e362, 2016.
13. Torkey HM, Abou-Yousef HM, Abdel Azeiz AZ and Hoda EA: Insecticidal effect of cucurbitacin E glycoside isolated from Citrullus colocynthis against Aphis craccivora. Aust J Basic Appl Sci 3: 4060-4066, 2009.
14. Ma G, Luo W, Lu J, Ma DL, Leung CH, Wang Y and Chen X: Cucurbitacin E induces caspase-dependent apoptosis and protective autophagy mediated by ROS in lung cancer cells. Chem Biol Interact 253: 1-9, 2016.
15. Feng H, Zang L, Zhao ZX and Kan QC: Cucurbitacin-E inhibits multiple cancer cells proliferation through attenuation of Wnt/β-catenin signaling. Cancer Biother Radiopharm 29: 210-214, 2014.
16. Hsu YC, Huang TY and Chen MJ: Therapeutic ROS targeting of GADD45γ in the induction of G2/M arrest in primary human colorectal cancer cell lines by cucurbitacin E. Cell Death Dis 5: e1198, 2014.
17. Kong Y, Chen J, Zhou Z, Xia H, Qiu MH and Chen C: Cucurbitacin E induces cell cycle G2/M phase arrest and apoptosis in triple negative breast cancer. PLoS One 9: e103760, 2014.
18. Zhang T, Li J, Dong Y, Zhai D, Lai L, Dai F, Deng H, Chen Y, Liu M and Yi Z: Cucurbitacin E inhibits breast tumor metastasis by suppressing cell migration and invasion. Breast Cancer Res Treat 135: 445-458, 2012.
19. Garg S, Kaul SC and Wadhwa R: Cucurbitacin B and cancer intervention: Chemistry, biology and mechanisms (Review). Int J Oncol 52: 19-37, 2018.
20. Johnson R and Halder G: The two faces of hippo: Targeting the hippo pathway for regenerative medicine and cancer treatment. Nat Rev Drug Discov 13: 63-79, 2014.
21. Zanconato F, Cordenonsi M and Piccolo S: YAP/TAZ at the roots of cancer. Cancer Cell 29: 783-803, 2016.
22. You B, Yang YL, Xu Z, Dai Y, Liu S, Mao JH, Tetsu O, Li H, Jablons DM and You L1: Inhibition of ERK1/2 down-regulates the Hippo/YAP signaling pathway in human NSCLC cells. Oncotarget 6: 4357-4368, 2015.
23. Ye XY, Luo QQ, Xu YH, Tang NW, Niu XM, Li ZM, Shen SP, Lu S and Chen ZW: 17-AAG suppresses growth and invasion of lung adenocarcinoma cells via regulation of the LATS1/YAP pathway. J Cell Mol Med 19: 651-663, 2015.
24. Hsu PC, You B, Yang YL, Zhang WQ, Wang YC, Xu Z, Dai Y, Liu S, Yang CT, Li H, *et al*: YAP promotes erlotinib resistance in human non-small cell lung cancer cells. Oncotarget 7: 51922-51933, 2016.
25. Janse van Rensburg HJ and Yang X: The roles of the hippo pathway in cancer metastasis. Cell Signal 28: 1761-1772, 2016.
26. Miao J, Hsu PC, Yang YL, Xu Z, Dai Y, Wang Y, Chan G, Huang Z, Hu B, Li H, *et al*: YAP regulates PD-L1 expression in human NSCLC cells. Oncotarget 8: 114576-114587, 2017.
27. Hsu PC, Miao J, Huang Z, Yang YL, Xu Z, You J, Dai Y, Yeh CC, Chan G, Liu S, *et al*: Inhibition of yes-associated protein suppresses brain metastasis of human lung adenocarcinoma in a murine model. J Cell Mol Med 22: 3073-3085, 2018.
28. Hsu PC, Yang CT, Jablons DM and You L: The role of yes-associated protein (YAP) in regulating programmed death-ligand 1 (PD-L1) in thoracic cancer. Biomedicines 6: E114, 2018.
29. Nguyen DX, Chiang AC, Zhang XH, Kim JY, Kris MG, Ladanyi M, Gerald WL and Massagué J: WNT/TCF signaling through LEF1 and HOXB9 mediates lung adenocarcinoma metastasis. Cell 138: 51-62, 2009.
30. Valiente M, Obenauf AC, Jin X, Chen Q, Zhang XH, Lee DJ, Chaft JE, Kris MG, Huse JT, Brogi E, *et al*: Serpins promote cancer cell survival and vascular co-option in brain metastasis. Cell 156: 1002-1016, 2014.
31. Kim J, McMillan E, Kim HS, Venkateswaran N, Makkar G, Rodriguez-Canales J, Villalobos P, Neggers JE, Mendiratta S, Wei S, *et al*: XPO1-dependent nuclear export is a druggable vulnerability in KRAS-mutant lung cancer. Nature 538: 114-117, 2016.
32. He C, Mao D, Hua G, Lv X, Chen X, Angeletti PC, Dong J, Remmenga SW, Rodabaugh KJ, Zhou J, *et al*: The hippo/YAP pathway interacts with EGFR signaling and HPV oncoproteins to regulate cervical cancer progression. EMBO Mol Med 7: 1426-1449, 2015.
33. Lan T, Wang L, Xu Q, Liu W, Jin H, Mao W, Wang X and Wang X: Growth inhibitory effect of cucurbitacin E on breast cancer cells. Int J Clin Exp Pathol 6: 1799-1805, 2013.
34. Wu YL, Zhang YJ, Yao YL, Li ZM, Han X, Lian LH, Zhao YQ and Nan JX: Cucurbitacin E ameliorates hepatic fibrosis in vivo and in vitro through activation of AMPK and blocking mTOR-dependent signaling pathway. Toxicol Lett 258: 147-158, 2016.

35. Chai Y, Xiang K, Wu Y, Zhang T, Liu Y, Liu X, Zhen W and Si Y: Cucurbitacin B inhibits the hippo-YAP signaling pathway and exerts anticancer activity in colorectal cancer cells. Med Sci Monit 24: 9251-9258, 2018.
36. Cai Y, Fang X, He C, Li P, Xiao F, Wang Y and Chen M: Cucurbitacins: A systematic review of the phytochemistry and anticancer activity. Am J Chin Med 43: 1331-1350, 2015.
37. Sun C, Zhang M, Shan X, Zhou X, Yang J, Wang Y, Li-Ling J and Deng Y: Inhibitory effect of cucurbitacin E on pancreatic cancer cells growth via STAT3 signaling. J Cancer Res Clin Oncol 136: 603-610, 2010.
38. Surmann-Schmitt C, Sasaki T, Hattori T, Eitzinger N, Schett G, von der Mark K and Stock M: The Wnt antagonist Wif-1 interacts with CTGF and inhibits CTGF activity. J Cell Physiol 227: 2207-2216, 2012.
39. Liu H, Peng F, Liu Z, Jiang F, Li L, Gao S, Wang G, Song J, Ruan E, Shao Z, et al: CYR61/CCN1 stimulates proliferation and differentiation of osteoblasts in vitro and contributes to bone remodeling in vivo in myeloma bone disease. Int J Oncol 50: 631-639, 2017.
40. Ren L, Wang X, Dong Z, Liu J and Zhang S: Bone metastasis from breast cancer involves elevated IL-11 expression and the gp130/STAT3 pathway. Med Oncol 30: 634, 2013.
41. Liao XH, Wang N, Liu LY, Zheng L, Xing WJ, Zhao DW, Sun XG, Hu P, Dong J and Zhang TC: MRTF-A and STAT3 synergistically promote breast cancer cell migration. Cell Signal 26: 2370-2380, 2014.
42. Singh A, Greninger P, Rhodes D, Koopman L, Violette S, Bardeesy N and Settleman J: A gene expression signature associated with 'K-Ras addiction' reveals regulators of EMT and tumor cell survival. Cancer Cell 15: 489-500, 2009.
43. Shao DD, Xue W, Krall EB, Bhutkar A, Piccioni F, Wang X, Schinzel AC, Sood S, Rosenbluh J and Kim JW: KRAS and YAP1 converge to regulate EMT and tumor survival. Cell 158: 171-184, 2014.
44. Kapoor A, Yao W, Ying H, Hua S, Liewen A, Wang Q, Zhong Y, Wu CJ, Sadanandam A, Hu B, et al: Yap1 activation enables bypass of oncogenic Kras addiction in pancreatic cancer. Cell 158: 185-197, 2014.
45. Greten FR: YAP1 takes over when oncogenic K-Ras slumbers. Cell 158: 11-12, 2014.